

Measured Temperature Dependence of Scintillation Camera Signals Read Out by Geiger–Müller Mode Avalanche Photodiodes

William C. J. Hunter, *Member, IEEE*, Robert S. Miyaoka, *Member, IEEE*, L. R. MacDonald, *Member, IEEE*, Thomas K. Lewellen, *Fellow, IEEE*

Abstract—We are developing a prototype monolithic scintillation camera with optical sensors on the entrance surface (SES) for use with statistically-estimated depth-of-interaction in a continuous scintillator. We opt to use Geiger–Müller mode avalanche photodiodes (GM-APDs) for the SES camera since they possess many desirable properties; for the intended application (SES and PET/MR imaging), they offer a thin attenuation profile and an operational insensitivity to large magnetic fields. However, one issue that must be addressed in using GM-APDs in an RF environment (as in MR scanners) is the thermal dissipation that can occur in this semiconductor material.

Signals of GM-APDs are strongly dependent on junction temperature. Consequently, we are developing a temperature-controlled GM-APD-based PET camera whose monitored temperature can be used to dynamically account for the temperature dependence of the output signals. Presently, we aim to characterize the output-signal dependence on temperature and bias for a GM-APD-based scintillation camera.

We've examined two GM-APDs, a Zecotek prototype MAPD-3N, and a SensL commercial SPMArray2. The dominant effect of temperature on gain that we observe results from a linear dependence of breakdown voltage on temperature (0.071 V/°C and 0.024 V/°C, respectively); at 2.3 V excess bias (voltage above breakdown) the resulting change in gain with temperature (without adjusting bias voltage) is -8.5% per °C for the MAPD-3N and -1.5 % per °C for the SPMArray2. For fixed excess bias, change in dark current with temperature varied widely, decreasing by 25% to 40% as temperature was changed from 20 °C to 10 °C and again by 20% to 35% going from 10 °C to 0 °C. Finally, using two MAPD-3N to read out a pair of 3.5-by-3.5-by-20 mm³ Zecotek LFS-3 scintillators in coincidence, we observe a decrease from 1.7 nsec to 1.5 nsec in coincidence-time resolution as we lowered temperature from 23 °C to 10 °C.

I. INTRODUCTION

A Geiger–Müller mode avalanche photodiode (GM-APD) is a micro-array of p-n junctions operated at a reverse bias in excess of its breakdown voltage ($V_{Ex} = V_{Bias} - V_{Brk}$); an active or passive circuit quenches the self-sustaining avalanche that would normally occur in a Geiger-mode device [1,2]. For a low photon flux (\ll junction density), the GM-APD output is (on average) proportional to the incident photon flux. In view of their high gain, fine time resolution, compact form, insensitivity to high magnetic fields, and their anticipated low cost, our lab is considering GM-APDs for future development of several PET detector systems.

We expect the gain of a GM-APD (a solid-state device) to be stable over time for a fixed bias and temperature. However, the p-n junction breakdown voltage (V_B) is strongly dependant on its temperature [3]. The output gain and other operating

characteristics that depend on the reverse bias in excess of V_B will therefore also depend on temperature.

The temperature in a GM-APD depends on several factors and may vary in time. The pulsed avalanche current can dissipate considerable power in the device (~Watts). The GM-APD operating temperature will therefore depend on the photon count rate, thermal resistance between diode and heat sink, and on ambient temperature. Therefore, it is important to monitor and stabilize the junction temperature.

II. MATERIALS AND METHODS

We examine the temperature-dependent signals of the two GM-APD arrays summarized in Table 1. With this data we will specify our temperature set point and control requirements for the development of a GM-APD-based scintillation camera.

Device	SPMArray2	MAPD-3N
Manufacturer	SensL	Zecotek
Pixel active area	2.8mm × 2.8mm	3mm × 3mm
Microcells/pixel	3,640	135,000
Number pixels	4 × 4	8 × 8
Microcell gain	< 10 ⁵	> 10 ⁶

Table 1. Manufacturer specifications of two GM-APDs that we examined.

A. Temperature-controlled dark box

We enclose each GM-APD in a temperature-controlled air-cooled optical-dark box (see Fig. 1). The optical dark box is a 30-by-36-by-16 cubic-inch gasket-sealed steel box fitted with light-tight signal and power-line connectors. This box was made large enough to include an existing 2D linear stage for remote source and collimator positioning. We insulated the dark box with two-inch-thick polystyrene and we made use of ventilated Peltier coolers and a PID-controlled power supply. We monitored temperature with a type-T thermocouple and a 0.1-°C-precision PID controller from Omega Engineering, Inc.

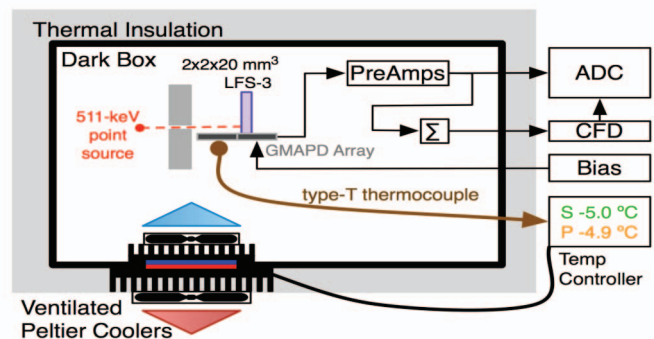


Fig. 1. Acquisition setup with optical and thermal isolation.

This work was supported in part by NIH grant EB002117, DOE grant DE-FG02-08ER64676, and Zecotek Photonics Inc.

B. Characterization of Zecotek MAPD-3N

We conducted preliminary measurements of the MAPD-3N while we were waiting for delivery of the SPMArray2 devices. The existing packaging for the MAPD-3N devices have a large attenuation profile and are not suited for SES readout.

We first measured dark current verses reverse bias voltage at several set temperatures; for this measurement, we used a series load (1.2 M Ω) and two digital multimeters (10.0 M Ω) that were connected from outside the dark box.

Next, we measured anode signals for a GM-APD that was optically coupled to one side of a $3.5 \times 3.5 \times 20$ mm³ scintillator. Signal spectra were acquired at different temperatures and GM-APD reverse bias voltages. A weak 511-keV point source (Ge-68) was used to avoid significant heating dissipation in the GM-APD; the detector count rate was less than 1 kHz. We used a polished LFS-3 scintillation crystal manufactured by Zecotek (a Lutetium-based scintillator, US patent No. 7,132,060) wrapped in four layers of Teflon tape. Signals were measured (Fig. 2) by a peak-sensing CAMAC analog-to-digital converter (ADC) through a spectral amplifier (500-nsec shaping) and triggered by a constant fraction discriminator (CFD).

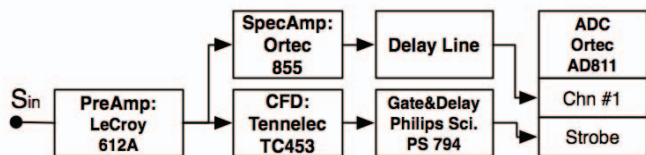


Fig. 2. MAPD-3N signal acquisition.

Finally, we measured coincidence time resolution using a similar second detector turned on its side to narrow the collimation depth in the primary detector (Fig. 3).

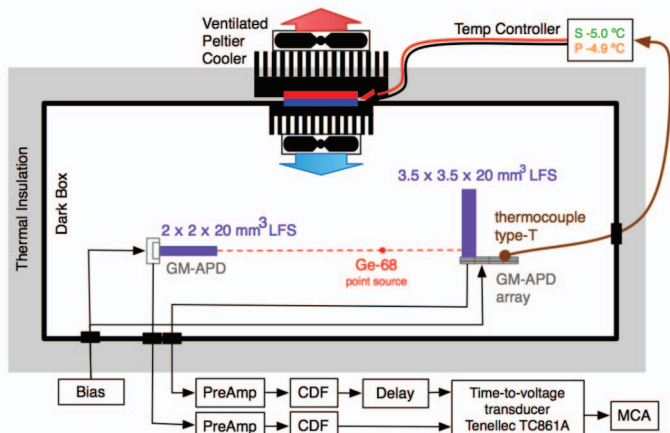


Fig. 3. Acquisition setup for GM-APD coincident time resolution.

C. Characterization of SensL SPMArray2

In our conceptual design of a PET/MR insert, we expect to air cool both, the detectors and data acquisition system. We therefore intend to measure the combined temperature dependence of the detector and preamplifiers (see Fig. 1).

Variations of gain with temperature for the SPMArray2 pixels were measured using collimated 511-keV gamma rays

from a 10- μ Ci ²²Na point source. A single 2x2x20mm³ LFS-3 scintillator (Lutetium-based scintillator by Zecotek) wrapped in four layers of Teflon tape was coupled to individual GM-APDs. Gain is computed as the mean photopeak position divided by 511 keV. We repeat this process for each pixel over a range of temperature and bias.

We read out SPMArray2 signals as shown in Fig. 4. The sixteen signals of a SPMArray2 are read out by a 16-channel SensL preamp board (SPMArray2-01). Differential signals are output by these preamp boards for subsequent pulse processing. At present, we also make use of the SensL evaluation board (SPMArray2-02) to convert differential to single ended signals and to output the signal sum for triggering the charge-integrating ADCs (QDC). Prior to use of these detectors as part of a PET/MR insert, we must change our pulse processing to include differential receives. The four 16-channel sums are then used to produce a common or-gate by a quad constant fraction discriminator (CFD). We are using a 400-nsec gate for the QDC acquisition.

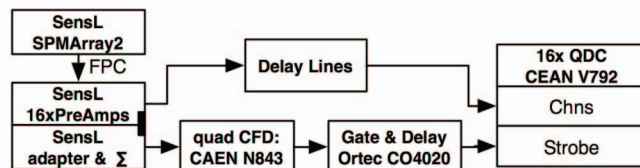


Fig. 4. SPMArray2 signal acquisition.

Dark current of the SPMArray2 was measured with the scintillator removed as a function of temperature and bias. For this purpose, we had to subtract a pixel-dependent baseline current that was observed at zero volts bias.

III. RESULTS

A. Zecotek MAPD-3N

We examine two pixels of a Zecotek MAPD-3N 8-by-8-pixel array: a corner pixel (A8) and an edge pixel (A3). Fig. 5 is an example of the pulse-height spectrum for an electronically collimated Ge-68 point source and a LFS-3 detector readout by a MAPD-3N. The photopeak mean position and full-width at half max (FWHM) are determined by log-matched filter of a Gaussian in a window about the photopeak (full-width at quarter-max).

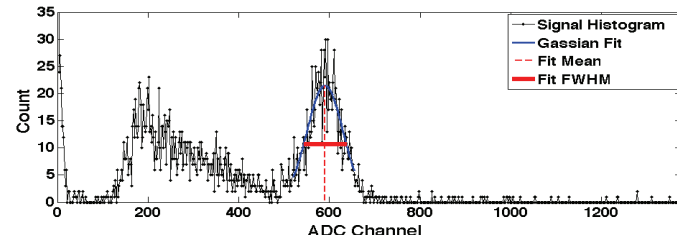


Fig. 5. Example of MAPD-3N signal histogram: chn. A3, 7.5 °C, 88.1 V.

In Fig. 6, we show measured photopeak position verses bias at several operating temperatures. Extrapolating to zero-mean signal, we can determine the breakdown voltage at each temperature. As the GM-APD heats up, breakdown voltage

increases: $\partial V_{\text{Brk}}/\partial T = 0.071 \text{ V}/^\circ\text{C}$. At 2.3 V excess bias for the prototype MAPD-3N, gain correspondingly changes with temperature at a relative rate of -8.5 % per $^\circ\text{C}$.

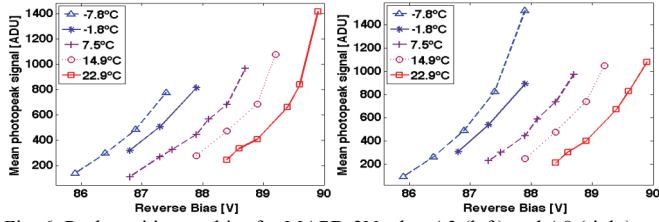


Fig. 6. Peak position vs. bias for MAPD-3N, chn. A3 (left) and A8 (right).

Fig. 7 shows a measure of energy resolution, given as the fitted FWHM over mean photopeak signal. Although fairly noisy, we observe a minor increase in energy resolution; for given excess bias, we observe a relative increase of 0.4% per $^\circ\text{C}$ in the photopeak FWHM-over-mean. This slow increase of energy resolution with temperature is reflective of the relatively large photodetector signal in one-to-one coupling of scintillator to GM-APD. For an arrayed readout of a monolithic scintillator, light sharing amongst GM-APDs will result in more-significant temperature dependence.

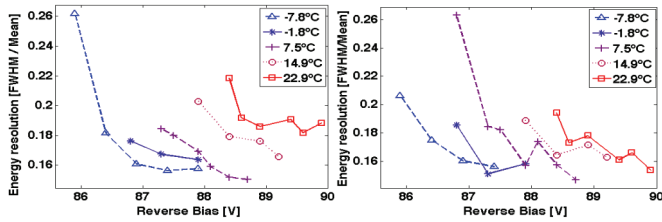


Fig. 7. FWHM/mean vs. bias for photopeak events of the MAPD-3N: channels A3 (left) and A8 (right). Connecting lines are a visual aid only.

Using the extrapolated breakdown voltages from Fig. 6, in Fig. 8 we show measured dark current of the MAPD-3N versus excess bias (applied minus breakdown voltage) for several temperatures.

In Fig. 9 we give an example of how we have measured coincidence time resolution. In Fig. 10 we summarize coincidence time resolution of the MAPD-3N vs. bias for several temperatures.

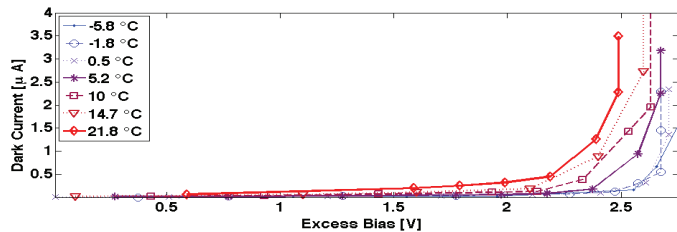


Fig. 8. Dark current verses excess bias for a channel A8 of the MAPD-3N.

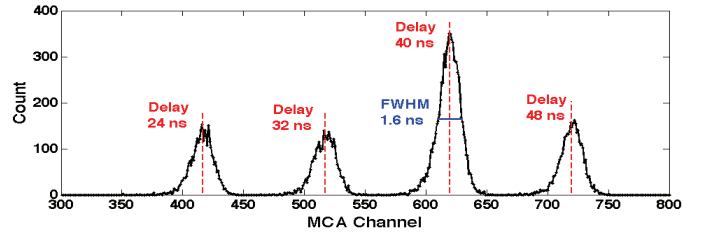


Fig. 9. Several known delays were used to convert the TC861A transducer response to time differences. Coincidence time resolution is then reported as the full-width at half-max for the best fit Gaussian at one time difference.

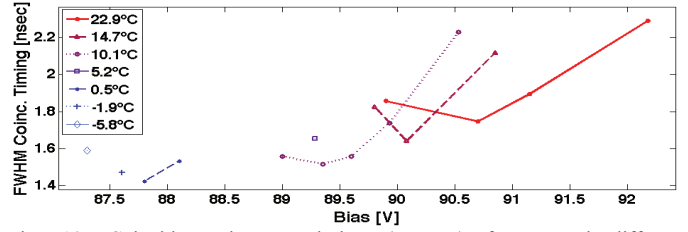


Fig. 10. Coincidence-time resolution (FWHM) for several different temperatures and biases for the MAPD-3N. We are presently acquiring more data at different bias voltages for the lower temperatures. However, we already observe a trend towards smaller FWHM at lower temperature (a decrease for the minimum FWHM of ~ 200 psec is observed when going from 23 $^\circ\text{C}$ to 10 $^\circ\text{C}$). We think this change is primarily attributed to the scintillator response although this hypothesis is untested.

B. SensL SPMArray2

The dependence of gain (G) for the SensL SPMArray2 on temperature (T) results from a nearly linear drift in V_{Brk} with temperature: $\partial V_{\text{Brk}}/\partial T = 0.024 \text{ V}/^\circ\text{C}$. The corresponding relative change in gain for the SPMArray2 at 2.3V excess bias is $\partial \ln(G)/\partial T = -1.5\% / ^\circ\text{C}$ (see Figs. 11 and 12). For fixed V_{Ex} , $\partial \ln(G)/\partial T$ is nearly constant with temperature.

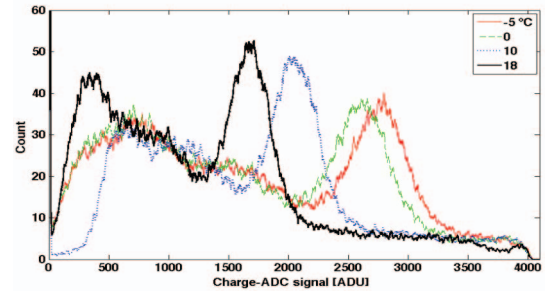


Fig. 11. Example of gain drift with temperature for the SPMArray2

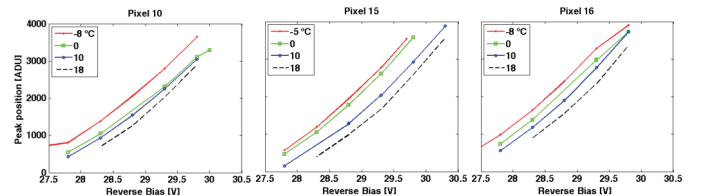


Fig. 12. Measured peak positions (pedestal subtracted) vs. bias voltage and temperature for three representative pixels of SPMArray2 GM-APD.

Dark current and dark current noise increase rapidly with bias voltage and temperature (see Fig. 13). For 2.3V fixed excess bias (V_{Ex}), change in dark current with temperature varied widely, decreasing by 25% to 40% as temperature was

changed from 20 °C to 10 °C and again by 20% to 35% as temperature was changed from 10 °C to 0 °C. This difference increases rapidly at higher V_{Ex} .

Using a single SPMArray2 per scintillation crystal, the noise we observe due to dark current (full-width at half max, FWHM) at ~20 °C is 1-2% of the signal amplitude. However, using an array of SPMArray2 to readout a block scintillator, the dark current noise will become the dominant source of signal variance (FWHM/mean > 20% from dark current alone).

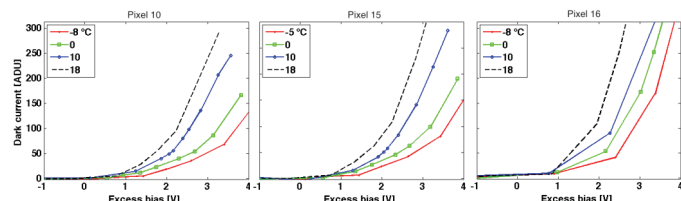


Fig. 13. Dark current dependence on bias voltage and temperature for the same three pixels of the SPMArray2 GM-APD (as in Fig. 12).

IV. CONCLUSIONS

We have found that temperature control should be better than 1.2°C for the SPMArray2 device and better than 0.2°C for the prototype MAPD-3N device to limit gain variance to less than 10% of the overall signal variance per pixel. Otherwise, using temperature dependent gain values may be of vital importance in gamma imaging.

Dark current is sufficiently low at room temperature (20 °C) for one-to-one readout for LFS-like scintillators for the two GM-APDs examined. However, use of a GM-APD array to readout a single LFS-like scintillator block will require cooling to 10°C or lower to significantly reduce dark current noise.

V. FUTURE DIRECTIONS

Having calibrated gains as a function of temperature, our next aim is to examine the benefit of dynamic gain adjustment to correct acquired data for temperature drift. The impact of this correction will be tested by comparing estimate variance and bias of detection parameters (position & energy) with and without dynamic gain adjustment.

VI. REFERENCES

[1] F. Zappa, S. Tisa, A. S. Cova, “Principles and features of single-photon avalanche diode arrays,” *Sens. Actuators, A*, vol. 140, pp. 103–112, 2007.
 [2] F. Zappa, S. Tisa, A. S. Cova, “Electronics for single photon avalanche diode arrays,” *Sens. Actuators, A*, vol. 140, pp. 113–122, 2007.
 [3] H. Dautet, et al. “Photon counting techniques with silicon avalanche photodiodes,” *Appl. Opt.*, vol. 32, no. 21, pp. 3894-3900, 1993.